JOURNAL OF SOLID STATE CHEMISTRY **123,** 30–38 (1996)
ARTICLE NO. 0148

Solid Solubility of Cerium in $BaTiO_3$

D. Makovec, Z. Samardžija, and D. Kolar

"J. Stefan" Institute, University of Ljubljana, Ljubljana, Slovenia

Received August 29, 1995; in revised form December 20, 1995; accepted December 21, 1995

Incorporation of Ce into the $BaTiO_3$ lattice was studied by quantitative wavelength dispersive spectroscopy–electron probe microanalysis (WDS/EPMA) in combination with scanning electron microscopy (SEM) and X-ray powder diffractometry (XRPD). The experimental results were used to decide among various theoretically possible formulas of Ce–$BaTiO_3$ solid solutions. Highly Ce-doped $BaTiO_3$ specimens, synthesized by mixed oxide technology, were prepared in ambient air or in a flow of a gas mixture of 92% Ar–8% H_2 at 1200 and 1400°C. When fired in air, cerium could be incorporated into the $BaTiO_3$ perovskite lattice as Ce^{4+} at Ti sites or/and as Ce^{3+} at Ba sites, depending on the starting composition. During firing in a reductive atmosphere Ce is incorporated exclusively as Ce^{3+} at the Ba sites. A broad solid solubility region between the $Ba_{1-X}Ce^{3+}_{X}Ti^{4+}_{1-X}Ti^{3+}_{X}O_3$ solution and the Ti-deficient $Ba_{1-X}Ce^{3+}_{X}Ti^{4+}_{1-X/4-2\delta}Ti^{3+}_{2\delta}(V_{Ti})_{X/4}O_{3-\delta}$ solution was detected. © 1996 Academic Press, Inc.

1. INTRODUCTION

Doped $BaTiO_3$ ceramics are widely used as materials for capacitors and resistors with a positive temperature coefficient of resistivity (PTCR). The dielectric and semiconducting properties of $BaTiO_3$ ceramics can be modified by additions of various ions, especially those which dissolve in the $BaTiO_3$ matrix. Among a wide variety of modifying ions cerium undoubtedly has a special place, because it could enter the perovskite $BaTiO_3$ lattice in oxidation state 4+ as well as in oxidation state 3+. From a comparison of the effective ionic radii of the ions involved (Table 1) (1), it may be predicted that Ce^{4+} should enter the $BaTiO_3$ lattice at octahedrally coordinated Ti sites, while Ce^{3+} should exchange with dodencahedrally coordinated Ba ions. Ce^{3+} incorporated at Ba sites acts as a donor dopant. Donor dopants have a higher valency than the substituted ions, and therefore their incorporation requires formation of effectively negatively charged defects, e.g., cation vacancies, anion interstitials, electrons, or acceptor impurities. The donor charge compensation mechanism in doped $BaTiO_3$ depends on the partial pressure of oxygen in the firing atmosphere and the donor concentration (2–14). Donor doped $BaTiO_3$, sintered in the reducing conditions of an atmosphere with a low oxygen partial pressure (for example in H_2), as well as $BaTiO_3$ doped with low donor concentrations (below approximately 0.5 mol%) and sintered in air, is semiconducting (2–5). It is generally accepted (2–5) that the semiconductivity of donor doped $BaTiO_3$ results from donor charge compensation by conduction electrons ($[D\cdot] = e'$). Alternatively, donor charge compensation may be expressed as a reduction of Ti^{4+} to Ti^{3+} and the solid solution can be described by the formula $Ba_{1-X}D^{3+}_{X}Ti^{4+}_{1-X}Ti^{3+}_{X}O_3$. At higher levels of donor dopant in $BaTiO_3$ ceramics sintered in air (above approximately 0.5 mol%), the donor charge compensation mechanism changes and the ceramics become insulating. Since interstitials are unfavorable defects in the $BaTiO_3$ structure with its high packing density (6), charge may be compensated by ionized vacancies in the cation sublattice. Some early works (7–9) proposed ionized Ba-site vacancies; however, nowadays it is known (3, 6, 10–14) that the donor charge in air-sintered, highly donor doped $BaTiO_3$ ceramics is compensated by ionized vacancies at the Ti sites (V''''_{Ti}). A solid solution of a three-valent dopant at Ba sites may be described by the formula $Ba_{1-X}D^{3+}_{X}Ti_{1-X/4}(V''''_{Ti})_{X/4}O_3$.

In the literature there are relatively few data on Ce-doped $BaTiO_3$. Guha and Kolar (16) determined a broad solid solubility region of Ce^{4+} in $BaTiO_3$ in their three-component phase diagram of the $BaO–CeO_2–TiO_2$ system. The solid solution extends along the tie-line between $BaTiO_3$ and $BaCeO_3$ to the approximate composition $BaTi_{0.6}Ce^{4+}_{0.4}O_3$ (1200°C in air). At high temperatures in an atmosphere with low oxygen partial pressure, CeO_2 would reduce to Ce_2O_3, while in air, cerium is relatively stable in its oxidation state 4+ (17). However, on the basis of the influence of CeO_2 doping on the electrical properties and microstructure of $BaTiO_3$ ceramics, it was concluded that Ce could also act as a donor dopant when CeO_2-doped $BaTiO_3$ is sintered in air (5, 18). In this case Ce^{4+} must be reduce to Ce^{3+}. Recently, reduction of CeO_2 during incorporation of Ce^{3+} into the $BaTiO_3$ lattice was proved by thermogravimetry (13, 14). Cerium is incorporated as Ce^{3+} into the $BaTiO_3$ lattice when CeO_2 is added to $BaTiO_3$ together with excess amount of TiO_2 (13, 14).

0022-4596/96 $18.00

TABLE 1
Effective Ionic Radii of Ba^{2+}, Ti^{4+}, Ce^{4+}, and Ce^{3+} in Different Coordination States (1)

Ion	Effective ionic radius (nm) *CN* 6	Effective ionic radius (nm) *CN* 12
Ba^{2+}	—	0.161
Ti^{4+}	0.0605	—
Ce^{4+}	0.087	0.114
Ce^{3+}	0.101	0.134

In this work the mode of cerium incorporation into the $BaTiO_3$ lattice was systematically studied as a function of the starting composition (ratio between added CeO_2, BaO, and TiO_2) and the sintering atmosphere (air, Ar/H_2), using quantitative wavelength dispersive spectroscopy–electron probe microanalysis (WDS/EPMA) in combination with X-ray powder diffractometry (XRPD) and scanning electron microscopy (SEM).

2. EXPERIMENTAL

Samples with different compositions, marked in the three-component diagram in Fig. 1 and listed in Table 2, were prepared by conventional mixed oxide technology. $BaTiO_3$ (Transelco 219-8, LOT 881191) was mixed with appropriate amounts of CeO_2 (Koch-Light Lab., 99.9%), TiO_2 (anatase modification, Fluka AG, >99%), and $BaCO_3$ (Ventron Alfa, 99.999%), pressed into tablets, and fired for a long period (~5 days) at 1400°C in ambient air or in a flow of the gas mixture of 92% Ar–8% H_2, with intermittent cooling, crushing, mixing, and pressing to promote homogeneity. Equilibrated samples were quenched.

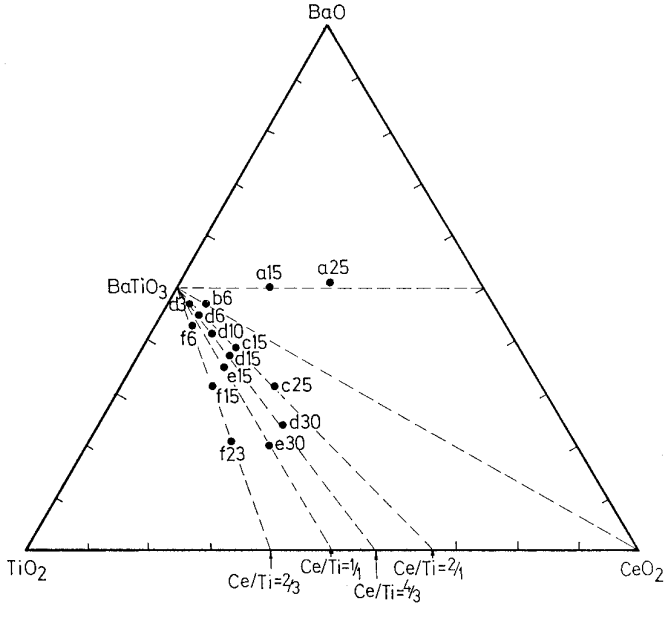

FIG. 1. The starting compositions analyzed are shown in the BaO–CeO_2–TiO_2 three-component diagram (16).

According to the manufacturer's analysis, $BaTiO_3$ Transelco 219-8, LOT 881191 contains a small excess of Ti (ratio Ba + Sr/Ti = 0.994).

Samples were analyzed by X-ray powder diffractometry (XRPD) (Model PW 1710, Netherlands Philips, Bedrijven b. v. S&I, The Netherlands) and by electron probe wavelength dispersive spectroscopic (WDS) microanalysis. Polished surfaces for microanalysis were prepared by conventional metallographic techniques. WDS microanalysis was performed on an electron probe microanalyzer (Model JXA 840A, JEOL, Tokyo, Japan) using TRACOR (Model TRACOR, Series II X-ray Microanalyzer, TRACOR, The Netherlands) software for quantitative analysis. The measurements of Ba, Ce, and Ti were carried out on a LiF crystal at 20 kV voltage, 15 nA electron beam current, and 40° take off angle. Counting times were sufficient to assure 1% relative counting deviation, resulting in good analytical sensitivity and precision. The calculated electron probe diameter for experimental conditions applied was below 150 nm. According to Monte Carlo electron trajectory simulation and Kanaya–Okayama electron range calculations (19), the excitation volume in the material analyzed was about 1 μm^3. The corresponding spatial resolution for WDS microanalysis was estimated to be less than 1 μm. Because of overlapping of the strongest Ce line ($CeL\alpha_{1,2}$) by the $BaL\beta_{1,4}$ line, a special calibration curve method (20, 21) was used in order to obtain correct results. In this method net counts per second (cps) for Ba were measured at the positions of the $BaL\alpha_1$ and $CeL\alpha_1$ lines in compounds with different Ba content, using $BaTiO_3$, $Ba_6Ti_{17}O_{40}$, and $BaTi_4O_9$. On the basis of these measurements, the calibration curve of net cps for Ba at the $CeL\alpha_1$ position versus net cps for Ba at the $BaL\alpha_1$ position was plotted. For analyzed phases (Ce-doped $BaTiO_3$) the net cps for Ce were determined by subtracting counts that were contributed by Ba. Corrected k ratios for Ce and measured k ratios for Ba and Ti were processed through the ZAF quantitative matrix procedure to obtain the corresponding element concentrations. Pure $BaTiO_3$ and CeO_2 were used as standards. A detailed consideration of the method used and the experimental conditions for WDS microanalysis has been published elsewhere (21).

3. RESULTS

3.1. Phase Composition

The phase composition of the samples was determined by diffractometry in combination with scanning microscopy and microanalysis. The results of X-ray diffractometry alone are not conclusive, since the peaks of coexisting

TABLE 2
Starting Compositions and Phases Determined after Firing at 1400°C in Ambient Air and in a Flow of 92% Ar–8% H_2 Gas Mixture

Sample	BaO mol%	CeO_2 mol%	TiO_2 mol%	PHASES DETERMINED[a] Sintering at 1400°C in air	Sintering at 1400°C in Ar/H_2 mixture
a15	50.00	15.00	35.00	BT_{ss}	BT_{ss}, B_2T_{ss}, CeO_2
a25	51.00	25.00	24.00	BT_{ss}, BC_{ss}, B_2T_{ss}	B_2T_{ss}, BT_{ss}
b6	47.00	6.00	47.00	BT_{ss}, CeO_2	BT_{ss}, B_2T_{ss}
c15	38.00	15.00	47.00		BT_{ss}, CeO_2
c25	31.25	25.00	43.75		BT_{ss}, CeO_2
d3	47.37	3.00	49.63	BT_{ss}	
d10	44.75	6.00	57.50	Bt_{ss}, BT_n, CeO_2	BT_{ss}
d15	36.88	15.00	48.12		BT_{ss}, B_2T_{ss}, CeO_2
d30	23.75	30.00	46.25		BT_{ss}, $B_2C_2T_5$, CT
e15	35.00	15.00	50.00		BT_{ss}
e30	20.00	30.00	50.00		BT_{ss}, CT_2
f6	42.50	6.00	51.50	BT_{ss}, BT_n, CeO_2	BT_{ss}, BT_n
f15	31.25	15.00	53.75		BT_{ss}, BT_n
f23	21.43	22.86	55.71		BT_{ss}, $BCT_{4(ss)}$, BT_n

[a] BT_{ss}: Ce-doped $BaTiO_3$, B_2T_{ss}: Ce-doped Ba_2TiO_4, BC_{ss}: Ti-doped $BaCeO_3$, BT_n: Ba-polytitanates, $BCT_{4(ss)}$: solid solution $BaCe_2Ti_4O_{12}$, $B_2C_2T_5$: $Ba_2Ce_4Ti_5O_{18}$, CT: Ce_2TiO_5, CT_2: $Ce_2Ti_2O_7$.

phases frequently overlap (for example, the peaks of $BaTi_4O_9$ and $BCT_{4(ss)}$) (for the meaning of the abbreviations see Table 2), or the single phases are too poorly crystalline (for example, all Ba-polytitanates). Results are summarized in Table 2.

Air-sintered samples, with compositions on and above the line which connects $BaTiO_3$ with CeO_2 (samples a15, a25, and b6) in the $BaO–CeO_2–TiO_2$ phase diagram (16) are of yellowish-gray color, whereas samples with composition below this lines (d10, f6) are orange.

Figure 2 shows the microstructures of the samples a25, b6, d3, and d10, sintered at 1400°C in ambient air. Sample a25 is composed of three phases (Ce-doped $BaTiO_3$, Ti-doped $BaCeO_3$, and Ce-doped Ba_2TiO_4), while sample b6 is composed of only two phases (Ce-doped $BaTiO_3$ and CeO_2). Sample d3 seems to be monophasic, while sample d10 is composed of Ce-doped $BaTiO_3$, CeO_2, and solidifed Ba-polytitanate melt. The Ba-polytitanate phase in samples d10 and f6 was analyzed by quantitative WDS microanalysis. The results suggest that the Ba-polytitanate phase is $Ba_6Ti_{17}O_{40}$ after firing at 1200°C and $BaTi_4O_9$ at 1400°C. The nature of Ba-polytitanate phase in these samples is in agreement with the $BaO–TiO_2$ phase diagram (22).

During sintering of samples in the reducing conditions of the mixture of 92% Ar–8% H_2, Ce^{4+} reduces to Ce^{3+}. All samples were black and semiconductive. It is known (4) that the dark color as well as the semiconductivity of $BaTiO_3$-based ceramics is related to the presence of Ti^{3+}. Figure 3 shows X-ray powder diffractograms of the samples d30, e30, and f23. The samples contain some Ce^{3+}-compounds, which are isostructural with compounds already known from other rare earth oxide (Ln_2O_3)–BaO–TiO_2 systems. In sample d30, Ce-doped $BaTiO_3$ is in equilibrium with a compound which is isostructural with the La-compound $Ba_2La_4Ti_5O_{18}$ (23), and with the compound Ce_2TiO_5 from the $Ce_2O_3–TiO_2$ binary system (24, 25). Sample e30 is composed of only two phases, Ce-doped $BaTiO_3$ and $Ce_2Ti_2O_7$. In the diffractogram of sample f23 (Fig. 3), only peaks of Ce-doped $BaTiO_3$ and $BCT_{4(ss)}$ solid solution are present, whereas, in the microstructure of this sample shown in Fig. 4, it is clearly evident that the sample is actually composed of three phases. The solid solution $BCT_{4(ss)}$ has a composition close to the atomic ratio Ba:Ce:Ti = 1:2:4 ($BaCe_2Ti_4O_{12}$) and is isostructural with the series of rare-earth solid solutions with compositions near $BaO \cdot Ln_2O_3 \cdot 4\ TiO_2$ (26, 27). Apart from two phases detected by diffractometry (Ce-doped $BaTiO_3$, $BCT_{4(ss)}$), a phase composed of only Ba, Ti, and O is present. WDS microanalysis performed on 10 crystallites of this phase showed the average composition 14.3 ± 0.8 mol% BaO, 85.7 ± 2.4 mol% TiO_x. Because of the reductive firing conditions, Ti could be partially in valency state 3+. This phase after quenching from the firing temperature obviously remained too poorly crystalline to be detected by diffractometry.

In the diffractograms of the samples a15, c15, c25, and d15, peaks of a phase with fluorite structure, ascribed to $CeO_{2-\delta}$, are visible. $CeO_{2-\delta}$ appears most probably as a

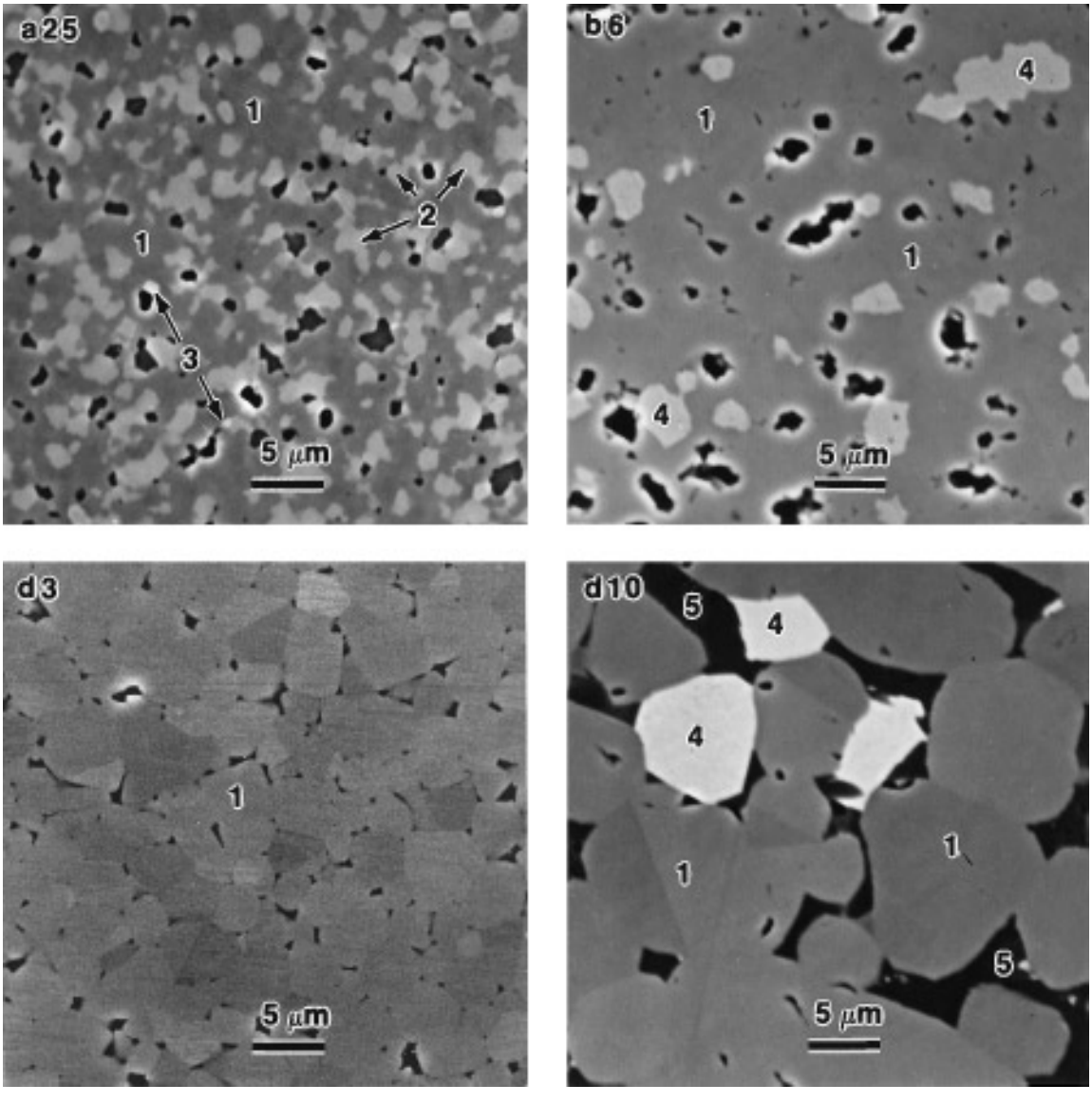

FIG. 2. Backscattered electron micrographs showing the microstructures of samples a25, b6, d3, and d10, sintered at 1400°C in air.

result of reaction between Ce_2O_3, formed during firing in the reductive conditions, and oxygen, when the pellets were exposed to ambient air. Ce_2O_3 is unstable in air even at room temperature (28).

Figure 5 shows the microstructures of the samples d10 and e15, fired at 1400°C in the flow of Ar/H_2. Both samples are monophasic.

3.2. Microanalysis of Ce-Doped $BaTiO_3$ Phase

In each chosen sample at least 10 Ce-doped $BaTiO_3$ grains were analyzed. Concentrations of Ba, Ce, and Ti were measured by quantitative WDS microanalysis. In Tables 3 and 5, results are given as average concentrations of each element with standard deviations obtained by statistical calculation of individual sets of results.

Results of microanalysis were then calculated to obtain perovskite formula ABO_3. For calculation of results of microanalysis to obtain the chemical formula, some clear and undoubted assumptions must be applied:

• $BaTiO_3$ has a very sharply defined composition. The solid solubility of both BaO or TiO_2 in $BaTiO_3$ is negligible (29, 30). Interstitial incorporation of atoms into the perovskite lattice is not likely to occur because of the perovskite's high packing density (6). The samples, fired in the reducing atmosphere, in which $BaTiO_3$ could be O deficient, are more problematic.

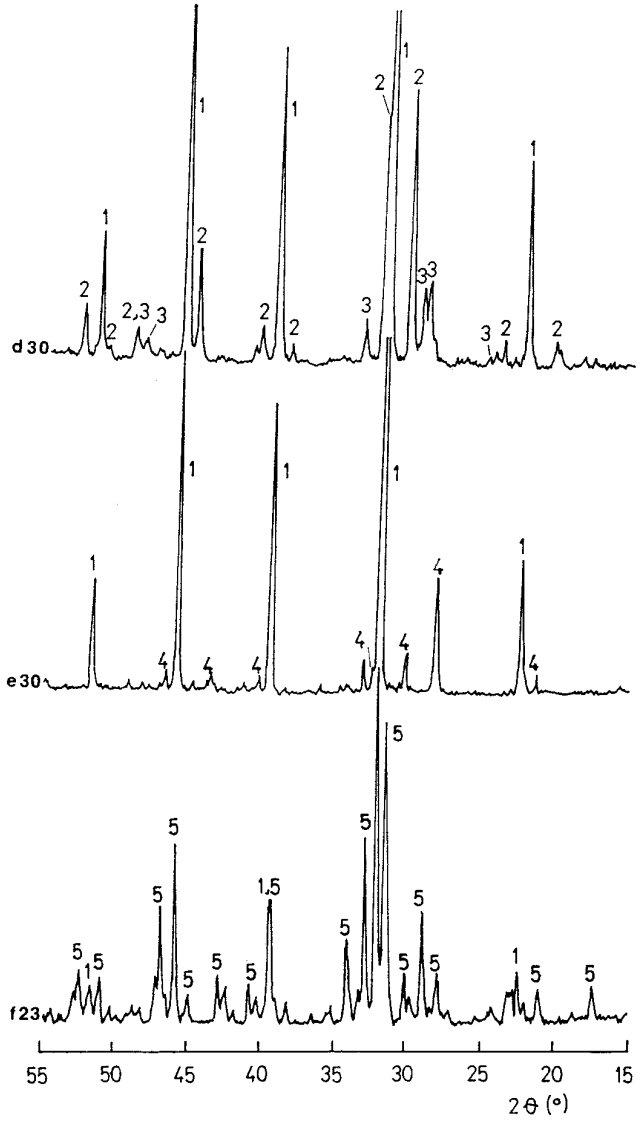

FIG. 3. X-ray powder diffractograms of samples d30, e30, and f23 fired at 1400°C in a flow of a 92% Ar–8% H_2 gas mixture. 1, Ce-doped $BaTiO_3$; 2, $Ba_2Ce_4Ti_5O_{18}$; 3, Ce_2TiO_5, 4, $Ce_2Ti_2O_7$; 5, $BaCe_2Ti_4O_{12}$ solid solution.

• The dopant is homogeneously distributed. The homogeneity of the phase analyzed was verified on the basis of the simplified criterion, widely used in X-ray counting statistics, that all the measured data must fall within $N \pm \sqrt{N}$ (average number of counts ± 3 standard counting deviations) (19). According to this criterion the Ce-doped $BaTiO_3$ phase was found to be homogeneous in all the samples analyzed.

• Ce could be incorporated exclusively as Ce^{4+} at Ti sites or as Ce^{3+} at Ba sites. This statement is in agreement with differences between the effective ionic radii of the cations involved (Table 1).

• Ce^{3+}-donor charge could be compensated by reduction of Ti^{4+} to Ti^{3+} (electronic compensation) by creation of ionized vacancies at Ti sites (V'''_{Ti}) or by a combination of both mechanisms (2, 3, 6, 10–15).

• Ce^{4+} and Ti^{3+} cannot coexist in the same solid solution. It was experimentally shown that Ce^{4+} reduces before Ti^{4+} (31).

If the assumptions listed are considered, five different types of solid solution are theoretically possible:

1. Ce is incorporated as Ce^{4+} at Ti sites, ($BaTi^{4+}_{1-x}Ce^{4+}_xO_3$).

2. Ce is incorporated as Ce^{3+} at Ba sites; excess charge is compensated by ionized vacancies at Ti sites, ($Ba_{1-X}Ce^{3+}_XTi^{4+}_{1-X/4}(V''''_{Ti})_{X/4}O_3$).

3. Ce is incorporated as Ce^{4+} at Ti sites and as Ce^{3+} at Ba sites; donor charge is compensated for by ionized vacancies at Ti sites, ($Ba_{1-X}Ce^{3+}_XTi^{4+}_{1-X/4-Y}Ce^{4+}_Y(V''''_{Ti})_{X/4}O_3$).

4. Ce is incorporated as Ce^{3+} at Ba sites; donor charge is compensated by reduction of Ti^{4+} to Ti^{3+}, ($Ba_{1-X}Ce^{3+}_XTi^{4+}_{1-X}Ti^{3+}_XO_3$).

5. Ce is incorporated as Ce^{3+} at Ba sites; donor charge is compensated by the combination of ionized vacancies and Ti^{3+}, ($Ba_{1-X}Ce^{3+}_XTi^{4+}_{1-X+3XY/4}Ti^{3+}_{X-XY}(V''''_{Ti})_{XY/4}O_3$; $0 < Y > 1$).

For measurement on every grain in an individual sample, measured concentrations were calculated to the theoretically possible formulas of solid solutions with normalization to three O per formula unit, taking into account the valency of an individual ion. Samples prepared by firing in the reducing atmosphere could be O deficient. If this is the case, a small systematic error is introduced, because of normalization to O.

For calculation of the results of microanalysis to the solid solution formulas, in which the measured element is

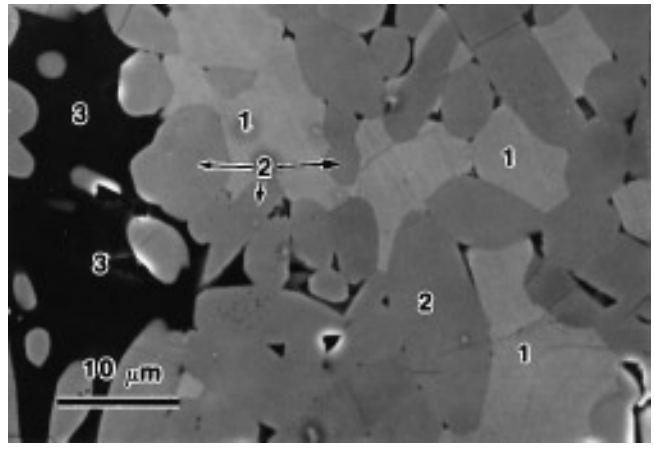

FIG. 4. Backscattered electron micrograph showing the microstructure of sample f23, fired at 1400°C in a flow of a 92% Ar–8% H_2 gas mixture.

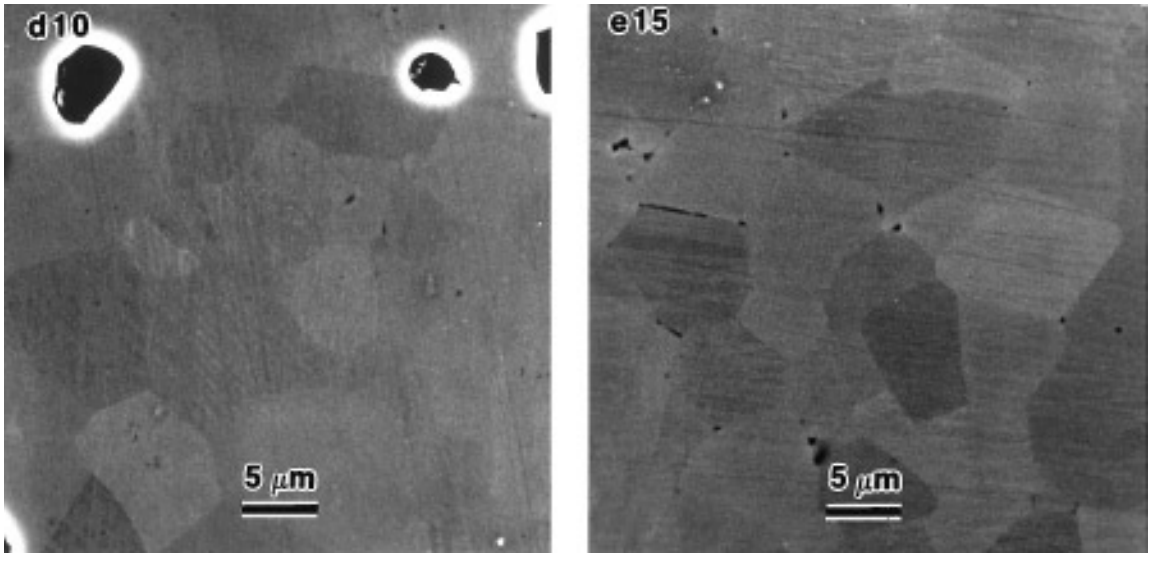

FIG. 5. Backscattered electron micrographs showing the microstructures of samples d10 and e15, fired at 1400°C in a flow of a 92% Ar–8% H_2 gas mixture. Both samples are monophasic.

present in two different oxidation states, the concentration of individual species was calculated using

$$[\mathrm{Ba}] + [\mathrm{Ce}^{3+}] = [\mathrm{Ti}^{4+}] + [\mathrm{Ce}^{4+}] + [\mathrm{Ti}^{3+}] + \left(\frac{[\mathrm{Ce}^{3+}] - [\mathrm{Ti}^{3+}]}{4}\right) \quad [1]$$

$$[\mathrm{Ce}^{4+}] + [\mathrm{Ce}^{3+}] = [\mathrm{Ce}] \quad [2]$$

$$[\mathrm{Ti}^{4+}] + [\mathrm{Ti}^{3+}] = [\mathrm{Ti}], \quad [3]$$

where [Ce] denotes the total element concentration and $[Ce^{4+}]$ denotes the concentration of the individual species.

Equation [1] postulates equivalent occupancy of A and B sites in the perovskite formula ABO_3. The A sites may be occupied by Ba^{2+} and Ce^{3+}, whereas at the B sites Ti^{4+}, Ce^{4+}, and species which compensate donor charge (V''''_{Ti} and Ti^{3+}) may be present. Each (V''''_{Ti}) compensates four Ce^{3+} ions and each Ti^{3+} one Ce^{3+}, incorporated at A sites.

In calculation of results to the presumed perovskite formulas only the ratios between ion concentrations were taken into account, and not the absolute values of measured concentrations. Consequently, some systematic errors in the microanalysis, which contribute relatively equally to the results of measurements for each element, were avoided. Systematic errors frequently arise during microanalysis because of microporosity, nonideal surface, etc. (19).

Chemical formulas, calculated from results of microanalysis at each point on an individual sample, were statistically treated to obtain average values and standard deviations of the coefficients in the formulas. The results of microanalysis of almost all samples match only one of the presumed theoretically possible solid solution formulas, taking into account the calculated standard deviations of the coefficients in the formulas. The calculated formulas, which match presumed theoretically possible formulas, are listed in Tables 4 and 6.

The Ce–$BaTiO_3$ solid solution in sample a25, fired at 1400°C in ambient air may be expressed by the formula $BaTi^{4+}_{1-X}Ce^{4+}_{X}O_3$. Solid solubility limit is at approximately $X \approx 0.35$. Of course, calculation of the results to the solid solution formulas cannot exclude the possibility that Ce^{3+} is also present in the solid solution at low concentrations, which are inside the deviations of the coefficients in the calculated formula.

Microanalysis of Ce-doped $BaTiO_3$ phase in samples d10 and f8, fired in ambient air, showed that the solid solution could be described by the formula $Ba_{1-X}Ce^{3+}_{X}Ti^{4+}_{1-X/4}(V''''_{Ti})_{X/4}O_3$. The solid solubility limit was around $X \approx 0.08$ at 1400°C and around $X \approx 0.04$ at 1200°C.

The solid solubility of Ce in $BaTiO_3$ in sample b6 is low. Because of the low concentration of Ce in $BaTiO_3$ and consequently the high deviations of the measurements, the results match two of the presumed theoretically possible formulas (listed in Table 4). The results fit the formula with Ce entirely in oxidation state 3+ ($Ba_{1-X}Ce^{3+}_{X}Ti^{4+}_{1-X/4}(V''''_{Ti})_{X/4}O_3$) and also the formula with Ce incorporated into the $BaTiO_3$ lattice in oxidation state 3+ and 4+ ($Ba_{1-X}Ce^{3+}_{X}Ti^{4+}_{1-X/4-Y}Ce^{4+}_{Y}(V''''_{Ti})_{X/4}O_3$).

Microanalysis of Ce-doped $BaTiO_3$ phase in the samples fired in flow of the 92% Ar–8% H_2 gas mixture confirmed that Ce is present exclusively in oxidation state 3+. The results obtained by microanalysis of samples a15, c15, and

TABLE 3
Results of Microanalysis of Samples Fired in Ambient Air at 1200°C and at 1400°C

Sample	T (°C)	Ba (at%)	Ce (at%)	Ti (at%)
a25	1400	19.51 ± 0.41	6.79 ± 0.43	12.31 ± 0.30
b6	1400	19.44 ± 0.40	0.54 ± 0.11	19.57 ± 0.54
d10	1400	17.55 ± 0.40	1.60 ± 0.07	18.66 ± 0.50
d10	1200	18.86 ± 0.39	0.82 ± 0.06	19.41 ± 0.35
f6	1400	16.99 ± 0.37	1.59 ± 0.06	18.45 ± 0.30

Note. Difference from 100 at% is O.

TABLE 5
Results of Microanalysis of Samples Fired in a Flow of 92% Ar–8% H_2 at 1400°C

Sample	Ba (at%)	Ce (at%)	Ti (at%)
a15	15.18 ± 0.43	5.98 ± 0.21	19.40 ± 0.30
c15	15.15 ± 0.41	5.54 ± 0.12	19.43 ± 0.31
d15	14.41 ± 0.25	5.96 ± 0.18	18.40 ± 0.47
d30	11.44 ± 0.33	8.40 ± 0.16	19.08 ± 0.39
e30	8.88 ± 0.72	10.91 ± 0.98	19.35 ± 0.34
f15	12.77 ± 0.30	6.95 ± 0.13	19.66 ± 0.44
f23	10.07 ± 0.53	10.39 ± 0.27	20.43 ± 0.26

Note. Difference from 100 at% is O.

d15 are equal and correspond to a formula with Ce^{3+} at Ba sites and a deficient Ti sublattice ($Ba_{1-X}Ce_X^{3+}Ti_{1-X/4}^{4+}(V_{Ti})_{X/4}O_3$). The solid solubility limit of this solid solution is at X around 0.28.

The solid solutions in samples e30, f15, and f23 may be described by a formula with Ce^{3+} at the Ba sites and fully occupied Ti sites. Donor charge is obviously compensated electronically by the reduction of Ti^{4+} to Ti^{3+} ($Ba_{1-X}Ce_X^{3+}Ti_{1-X}^{4+}Ti_X^{3+}O_3$). Grains of solid solution in sample e30 are relatively very small and unfavorable for microanalysis. Consequently, the standard deviations of the measurements of this sample are relatively high. The results are equal (considering the deviations) to results obtained on sample f23, which was more suitable for microanalysis. The solid solubility limit for this sample at 1400°C is very high (around a composition with $X \approx 52$ in the formula $Ba_{1-X}Ce_X^{3+}Ti_{1-X}^{4+}Ti_X^{3+}O_3$).

The results of microanalysis of sample d30 correspond to a formula with Ce^{3+} donor charge compensated by Ti^{3+}, as well as by vacancies at Ti sites ($Ba_{1-X}Ce_X^{3+}Ti_{1-X+3XY/4}^{4+}Ti_{X-XY}^{3+}(V_{Ti}'''')_{XY/4}O_3$).

4. DISCUSSION

With fitting the results of quantitative microanalysis to theoretically possible formulas of Ce–$BaTiO_3$ solid solutions using some reasonable assumptions, we were able to determine indirectly not only the solid solubility limits, but also the sites in perovskite lattice where the dopant is incorporated, its oxidation state, and donor charge compensation mechanism.

The mode of incorporation of Ce into the $BaTiO_3$ lattice at a particular temperature depends on the partial pressure of oxygen in the firing atmosphere and on starting composition.

In a firing atmosphere with a high oxygen partial pressure (air), cerium is preferentially in oxidation state 4+; however, in $BaTiO_3$ it may also be dissolved in oxidation state 3+. If CeO_2 is added to $BaTiO_3$ together with an excess amount of BaO, Ce will be incorporated preferentially as Ce^{4+} at Ti sites. The solid solution with the highest concentration of Ce^{4+} extends along the $BaTiO_3$–$BaCeO_3$ tie-line, at 1400°C to the composition approximately $BaTi_{0.65}Ce_{0.35}^{4+}O_3$ (around 18 mol% of CeO_2 is dissolved in $BaTiO_3$). The solid solubility limit is in good agreement with results obtained on the basis of XRPD by Guha and Kolar (16). They found that at 1200°C ~20 mol% of CeO_2 dissolved in $BaTiO_3$.

When CeO_2 is added to $BaTiO_3$ together with an excess amount of TiO_2, Ce is incorporated into the $BaTiO_3$ lattice as Ce^{3+} at the Ba sites. Monophasic samples are obtained

TABLE 4
Formulas of Ce–$BaTiO_3$ Solid Solutions, Calculated from Results of Microanalysis of Samples Fired in Ambient Air at 1200°C and at 1400°C

Sample	T (°C)	Calculated formula
a25	1400	$Ba_{1.015\pm0.017}Ti_{0.640\pm0.013}Ce_{0.353\pm0.019}^{4+}O_3$
b6	1400	$Ba_{0.981\pm0.007}Ce_{0.019\pm0.006}^{3+}Ti_{0.986\pm0.005}Ce_{0.008\pm0.005}^{4+}(V_{Ti}'''')_{0.005\pm0.001}O_3$
		$Ba_{0.981\pm0.008}Ce_{0.027\pm0.005}^{3+}Ti_{0.987\pm0.009}(V_{Ti}'''')_{0.007\pm0.001}O_3$
d10	1400	$Ba_{0.920\pm0.009}Ce_{0.084\pm0.004}^{3+}Ti_{0.978\pm0.007}(V_{Ti}'''')_{0.021\pm0.001}O_3$
d10	1200	$Ba_{0.958\pm0.013}Ce_{0.042\pm0.003}^{3+}Ti_{0.986\pm0.010}(V_{Ti}'''')_{0.011\pm0.001}O_3$
f6	1400	$Ba_{0.910\pm0.021}Ce_{0.085\pm0.003}^{3+}Ti_{0.984\pm0.005}(V_{Ti}'''')_{0.021\pm0.001}O_3$

TABLE 6
Formulas of Ce–$BaTiO_3$ Solid Solutions Calculated from Results of Microanalysis of Samples Fired in a Flow of 92% Ar–8% H_2

Sample	Calculated formula
a15	$Ba_{0.723\pm0.014}Ce_{0.285\pm0.013}^{3+}Ti_{0.925\pm0.011}^{4+}(V_{Ti})_{0.071\pm0.003}O_3$
c15	$Ba_{0.731\pm0.012}Ce_{0.267\pm0.008}^{3+}Ti_{0.937\pm0.009}^{4+}(V_{Ti})_{0.067\pm0.002}O_3$
d15	$Ba_{0.719\pm0.012}Ce_{0.296\pm0.006}^{3+}Ti_{0.918\pm0.006}^{4+}(V_{Ti})_{0.074\pm0.002}O_3$
d30	$Ba_{0.576\pm0.009}Ce_{0.424\pm0.009}^{3+}Ti_{0.715\pm0.066}^{4+}Ti_{0.268\pm0.045}^{3+}(V_{Ti})_{0.039\pm0.014}O_3$
e30	$Ba_{0.448\pm0.041}Ce_{0.550\pm0.038}^{3+}Ti_{0.507\pm0.036}^{4+}Ti_{0.450\pm0.077}^{3+}O_3$
f15	$Ba_{0.646\pm0.005}Ce_{0.352\pm0.005}^{3+}Ti_{0.656\pm0.022}^{4+}Ti_{0.340\pm0.033}^{3+}O_3$
f23	$Ba_{0.487\pm0.016}Ce_{0.516\pm0.011}^{3+}Ti_{0.465\pm0.026}^{4+}Ti_{0.533\pm0.033}^{3+}O_3$

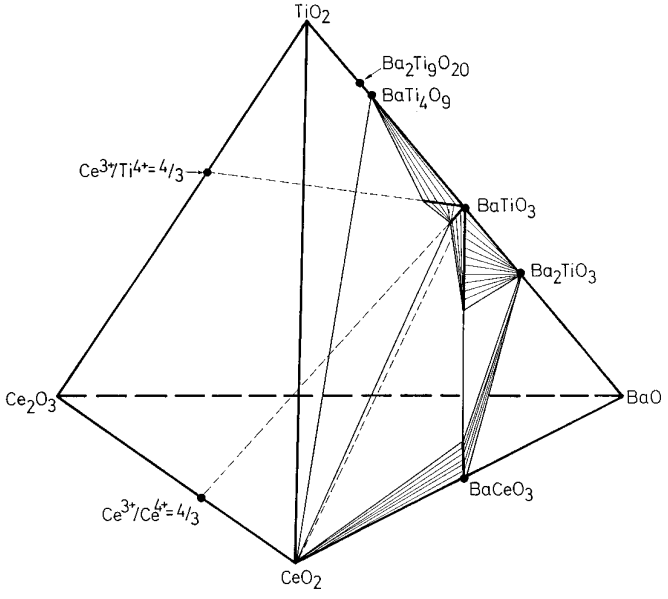

FIG. 6. Sketch of the phase diagram of the $BaO–CeO_2–Ce_2O_3–TiO_2$ system (1400°C in air).

when CeO_2 is added to $BaTiO_3$ together with TiO_2 in the molar ratio $CeO_2/TiO_2 = 4:3$ (sample d3 in Fig. 2). Donor charge is compensated by creation of ionized vacancies at the Ti sites. Reduction of CeO_2 during firing of the mixture of $BaTiO_3$, CeO_2, and TiO_2 in air was confirmed by thermogravimetry (13, 14). The solid solubility limit is strongly temperature dependent.

In the sample in which only CeO_2 was added to $BaTiO_3$ (sample b6) the solid solubility of Ce was relatively low. Consequently, the results of microanalysis could not be classified according to only one presumed solid solution formula. However, since this sample is composed only of two phases, Ce-doped $BaTiO_3$ and CeO_2 (Fig. 2), Ce must be incorporated into the $BaTiO_3$ lattice as Ce^{4+} as well as Ce^{3+}. If Ce were dissolved exclusively as Ce^{3+}, an additional Ti-rich phase would have appeared. To obtain solid solution which lies on the $BaTiO_3–CeO_2$ tie-line, Ce must be incorporated into the $BaTiO_3$ lattice as Ce^{3+} and as Ce^{4+} in the ratio $Ce^{3+}/Ce^{4+} = 4:3$, enabling Ce^{3+}-donor charge compensation by ionized vacancies at the Ti sites. The solid solution can be described by the formula $Ba_{1-4X/7}Ce^{3+}_{4X/7}Ti^{4+}_{1-3X/7}Ce^{4+}_{3X/7}(V''''_{Ti})_{X/7}O_3$. Results of microanalysis of the sample b6 are in agreement with such a mode of Ce incorporation. $Ce–BaTiO_3$ solid solutions are sketched in the $BaO–CeO_2–Ce_2O_3–TiO_2$ phase diagram in Fig. 6.

If a mixture of $BaTiO_3$, CeO_2, TiO_2, and BaO is fired in the reducing atmosphere of a gas mixture of 92% Ar–8% H_2, CeO_2 reduces and Ce is incorporated into the $BaTiO_3$ lattice as Ce^{3+}, independent of the starting composition. It is generally accepted (2–6, 14) that under reducing conditions of low oxygen partial pressure and high temperature, the donor charge is compensated by reduction of Ti^{4+} to Ti^{3+}. Fitting of the results of microanalysis to presumed theoretically possible formulas of the solid solutions showed that the Ce^{3+}-donor charge is undoubtedly compensated by Ti^{3+}, if enough Ti is present in the system. A $Ba_{1-X}Ce^{3+}_X Ti^{4+}_X Ti^{3+}_X O_3$ solid solution was formed when CeO_2 was added to $BaTiO_3$ together with an excess amount of TiO_2 in a molar ratio equal or higher than $CeO_2/TiO_2 = 1:1$ (samples e15, e30, f15, f30). However, if CeO_2 is added to $BaTiO_3$ together with an excess amount of BaO or TiO_2 at a molar ratio CeO_2/TiO_2 of less than 4:3 (samples a15, c15), a Ti-deficient solid solution is formed. The results of microanalysis fit the presumed formula $Ba_{1-X}Ce^{3+}_X Ti^{4+}_{1-X/4}(V_{Ti})_{X/4}O_3$; however, Ti^{3+} is also present since the samples are black in color. The results of microanalysis determine the compensation mechanism indirectly, taking into account some assumptions (in the calculations of solid solution formulas the results were normalized to 3 O per formula unit). Microanalysis confirmed that the Ti sublattice is deficient in accordance with the formula $Ba_{1-X}Ce^{3+}_X Ti^{4+}_{1-X/4}(V_{Ti})_{X/4}O_3$, whereas it cannot be said whether compensating electrons are localized at vacancies or not. If the donor charge was also compensated electronically in this Ti-deficient solution, then the O sublattice should also be deficient. In this case the Ti-deficient solution of $Ba_{1-X}Ce^{3+}_X Ti^{4+}_{1-X/4}(V''''_{Ti})_{X/4}O_3$ (determined on the basis of microanalysis) can be described by the formula $Ba_{1-X}Ce^{3+}_X Ti^{4+}_{1-X/4-2\delta}Ti^{3+}_{2\delta}(V_{Ti})_{X/4}O_{3-\delta}(V_O)_\delta$. If the entire Ce^{3+}-donor charge were compensated by Ti^{3+} then the value of δ is $X/2$, and if the donor charge were compensated by ionized vacancies at Ti sites then the value of δ is 0.

If the molar ratio between added CeO_2 and TiO_2 is equal to 4:3 (samples d15, d30), then a Ti-deficient solid solution of $Ba_{1-X}Ce^{3+}_X Ti^{4+}_{1-X/4-2\delta}Ti^{3+}_{2\delta}(V_{Ti})_{X/4}O_{3-\delta}(V_O)_\delta$ is formed, when the concentration of Ce^{3+} in the solid solution is below the solubility limit. On further additions of CeO_2 and TiO_2 in the ratio 4:3, titanium ions are incorporated into the lattice to a greater extend than Ce^{3+} ions so that the Ti deficiency is decreased.

The solubility limit of $Ba_{1-X}Ce^{3+}_X Ti^{4+}_{1-X}Ti^{3+}_X O_3$ solid solution is much higher ($X \sim 0.52$) than the solubility limit of $Ba_{1-X}Ce^{3+}_X Ti^{4+}_{1-X/4-2\delta}Ti^{3+}_{2\delta}(V_{Ti})_{X/4}O_{3-\delta}(V_O)_\delta$ solution ($X \sim 0.28$). Obviously, formation of a solution with a fully occupied Ti sublattice is favored during firing in a reductive atmosphere over formation of a Ti-deficient solution. If Ti is present in the system in excess with respect to the nominal formula $Ba_{1-x}Ce^{3+}_x Ti^{4+}_{1-x/4}(V_{Ti})_{x/4}O_3$, then the deficiency of the Ti sublattice is decreased. Decrease of the deficiency in the Ti sublattice is accompanied by increase in the solubility of Ce^{3+}.

5. CONCLUSIONS

The site at which cerium is incorporated at high temperatures in the barium titanate perovskite lattice depends on the oxygen partial pressure and starting composition.

• When sintered in air, Ce may be incorporated as Ce^{4+} at the Ti sites as well as Ce^{3+} at the Ba sites. When CeO_2 is added to $BaTiO_3$ with an excess amount of BaO, cerium is incorporated preferentially at the Ti sites. The solid solution at 1400°C extends along the $BaTiO_3$–$BaCeO_3$ tieline to the composition $BaTi_{0.65}Ce_{0.35}O_3$. When CeO_2 is added with an excess amount of TiO_2, cerium enters the $BaTiO_3$ lattice as Ce^{3+} at the Ba sites. The solid solubility of the $Ba_{1-x}Ce_x^{3+}Ti_{1-x/4}^{4+}(V_{Ti}'''')_{x/4}O_3$ solution is highly affected by the temperature. At 1400°C in air ~8 mol% of Ba ions are substituted by Ce^{3+} ions and at 1200°C ~4 mol% are substituted. When pure CeO_2 is added to $BaTiO_3$, the solid solubility is low. Cerium is incorporated into the $BaTiO_3$ lattice at Ba and Ti sites in the ratio of 4:3 ($Ba_{1-4X/7}Ce_{4X/7}^{3+}Ti_{1-3X/7}^{4+}Ce_{3X/7}^{4+}(V_{Ti}'''')_{X/7}O_3$).

• When samples are sintered in a reducing atmosphere (92% Ar–8% H_2), Ce is incorporated into the $BaTiO_3$ lattice as Ce^{3+} independent of the starting compositions. If CeO_2 is added to $BaTiO_3$ together with an excess amount of TiO_2 in a CeO_2/TiO_2 molar ratio equal to or higher than 1:1, a $Ba_{1-X}Ce_X^{3+}Ti_{1-X}^{4+}Ti_X^{3+}O_3$ solid solution is formed. If the concentration of Ti in the system is lower than required by this formula, then a Ti-deficient solid solution is formed. The solid solubility limit of the $Ba_{1-X}Ce_X^{3+}Ti_{1-X}^{4+}Ti_X^{3+}O_3$ solution is at $X \sim 0.52$ (1400°C), whereas solubility of the Ti-deficient solution ($Ba_{1-X}Ce_X^{3+}Ti_{1-X/4-2\delta}^{4+}Ti_{2\delta}^{3+}(V_{Ti})_{X/4}O_{3-\delta}(V_O)_\delta$) is much lower ($X \sim 0.28$ at 1400°C).

ACKNOWLEDGMENTS

This publication is based on work sponsored by the U.S.–Slovene Science and Technology Joint Fund in cooperation with Ministry of Science and Technology of Slovenia under Project NIST 95-351. We thank S. Zupančič for helping run the kilns.

REFERENCES

1. R. D. Shannon, *Acta. Crystallogr. A* **32,** 751 (1976).
2. W. D. Johnston and D. Sestrich, *J. Inorg. Nucl. Chem.* **20,** 32 (1961).
3. G. H. Jonker and E. E. Havinga, *Mater. Res. Bull.* **17,** 345 (1982).
4. E. J. W. Verwey, P. W. Haaymann, F. C. Romeijn, and G. W. Van Oosterhout, *Philips Res. Rep.* **5**(6), 173 (1950).
5. O. Saburi, *J. Phys. Soc. Jpn.* **14**(9), 1169 (1959).
6. G. V. Lewis and C. R. Catlow, *J. Phys. Chem. Solids* **47**(1), 89 (1986).
7. E. C. Subbarao and G. Shirane, *J. Am. Ceram. Soc.* **42,** 279 (1959).
8. G. A. Smolenski, V. A. Isupov, and A. I. Granovskaya, *Fiz. Tverd. Tela* **1**(10), 1573 (1959).
9. J. Daniels and K. Herdtl, *Philips Res. Rep.* **31,** 487 (1976).
10. H. M. Chan, M. P. Harmer, and D. M. Smyth, *J. Am. Ceram. Soc.* **69**(6), 507 (1986).
11. A. S. Shaikh and R. W. Vest, *J. Am. Ceram. Soc.* **69**(9), 689 (1986).
12. J. M. Millet, R. S. Roth, L. T. Ettlinger, and H. S. Parker, *J. Solid State Chem.* **67,** 257 (1987).
13. D. Makovec, Z. Samardžija, and D. Kolar, *in* "Third Euro—Ceramics, Vol. 1, Processing of Ceramics" (P. Duran and J. F. Fernandez, Eds.), p. 961. Faenza Editrice Iberica, Castellon de la Plana, 1993.
14. D. K. Hennings, B. Schreinemacher, and H. Schreinemacher, *J. Eur. Ceram. Soc.* **13,** 81 (1994).
15. D. Makovec, Z. Samardžija, U. Delalut, and D. Kolar, *J. Am. Ceram. Soc.* **78**(8), 2193 (1995).
16. J. P. Guha and D. Kolar, *J. Am. Ceram. Soc.* **56**(1), 5 (1973).
17. R. S. Roth, T. Negas, H. S. Parker, D. B. Minor, and C. Jones, *Mater. Res. Bull.* **12,** 1173 (1977).
18. L. A. Xue, Y. Chen, and R. J. Brook, *J. Mater. Sci.* **7,** 1163 (1988).
19. E. Goldstein *et al.*, "Scanning Electron Microscopy and X-Ray Microanalysis." Plenum Press, New York, 1992.
20. M. Čeh, Z. Samardžija, and D. Makovec, *Proc. Issue Scanning Supplement III* **15,** 94 (1993).
21. Z. Samardžija, M. Čeh, D. Makovec, and D. Kolar, *Mikrochim. Acta*, in press.
22. T. Negas, R. S. Roth, H. S. Parker, and D. Minor, *J. Solid State Chem.* **9,** 287 (1981).
23. V. A. Saltikova, O. V. Meljnikova, N. V. Leonova, and F. N. Fedorov, *Zh. Neorg. Khim.* **30**(1), 190 (1985).
24. I. M. Majster, A. V. Šavčenko, and L. M. Lopato, *Neorg. Mater.* **18,** 1589 (1982).
25. A. Prauss and R. Guehn, *J. Solid State Chem.* **110,** 363 (1994).
26. E. S. Razgon, A. M. Gens, M. B. Varfolomeev, S. S. Korovin, and V. S. Kostomarov, *Zh. Neorg. Khim.* **25**(8), 2298 (1980).
27. D. Kolar, S. Gaberšček, B. Volavšek, H. S. Parker, and R. S. Roth, *J. Solid State Chem.* **38,** 158 (1981).
28. R. C. Weast, Ed., "Handbook of Chemistry and Physics," 55th ed., B-80. CRC Press, Cleveland, Ohio, 1974–1975.
29. Y. H. Hu, M. P. Harmer, and D. M. Smith, *J. Am. Ceram. Soc.* **68**(7), 372 (1985).
30. R. K. Sharma, N. H. Chan, and D. M. Smith, *J. Am. Ceram. Soc.* **64**(8), 448 (1981).
31. A. J. Leonov, M. I. Piryutko, and E. K. Keller, *Bull. Akad. Nauk USSR Div. Chem. Sci.* (*Engl. Trans.*) **5,** 756 (1966).